

We would like to thank the topic editor for his suggestions. We address these specific points below:

**Topic Editor**

*I believe that the authors have made sufficient efforts to respond to the comments of the reviewers and that the paper can now be published. However, I would comment on two points raised by the reviewers.*

*While I agree with the authors in their comment on a question from Reviewer 1 that all is needed for Fig 4 is to show a measurable change in response, it would be good to add the changes in concentration used either in the text or in the figure caption. That both gases give an observable change at the same time is important, but the fact that the instrument gives the same result for such different concentrations of CO<sub>2</sub> and DMS is also of interest to potential users.*

*Reviewer 2's point about the changes in fluorescence shown in Fig 9 and discussed in the text on p 18, lines 11-12 is well taken, but is not really resolvable without taking samples for chlorophyll measurement. Fluorescence quenching is certainly well-known, but there can also be changes in chlorophyll over short vertical distances. Perhaps the DMS concentrations can help here. Is there any evidence that increased DMS production occurs at higher light levels? This could tip the balance towards the authors' contention that fluorescence quenching is occurring here.*

*If the authors can make these very minor changes, the paper can then be published and I do not need to see it again.*

*We have now adjusted the caption of Figure 4 and now state the initial and final concentrations used to determine the response time. The sentence now reads. 'Step changes from 350 to 400  $\mu$ atm for CO<sub>2</sub> and 0 to 2 nmol L<sup>-1</sup> for DMS have been scaled down so that the initial and end concentrations are between 0 and 1.'*

*We agree that without chlorophyll data our comments were speculative, we have now changes the text accordingly so we are no longer categorically stating that the change chlorophyll is definitely the result of quenching. The text now reads 'The increase in fluorescence with depth (Fig. 9c) is either due to reductions in chlorophyll concentration close to the sea surface or because of quenching of the phytoplankton photosynthetic apparatus, which is often observed in surface waters that experience strong irradiance (Sackmann et al., 2008).'*

We thank all 3 reviewers for their positive and constructive comments. We address their specific points below:

**Anonymous - reviewer 3**

*General comments*

*This paper reports on a near surface profiler for sampling biogeochemical properties of seawater near the surface, where important biological and air-sea exchange processes take place, and where*

vertical characterization has proved difficult. The motivation in developing this profiling device would be to study the effect of stratification on the biogeochemistry at the air-sea interface. There is no doubt that the authors have invested tremendous effort in developing and deploying the NSOP. However, I am a little disappointed with the scientific conclusions. In fact the article appears to be more of a technical description of an instrument, and therefore I think it might have been more appropriate for a more technical journal such as *Methods in Oceanography*. Therefore if the authors wish to publish this in *OS*, I suggest that they provide some further material on the scientific consequences of the NSOP. I do not think that this will require much effort, and although my major revisions rating appear to be a little severe, I do not think it will require much effort. The current effort in their conclusions - "The presence or absence of chemical and biological gradients within near surface stratified layers has been difficult to assess. NSOP is a platform with the capability to successfully resolve gradients in these near surface layers." - is weak, and I have no doubt that given the list of authors here, a little more effort would provide much improved conclusions. For example: how well does the temperature- $p\text{CO}_2$  relationship of 4.23% per degC hold? What are the global consequences for stratification on air-sea gas exchange?

We respectfully disagree with the reviewer. There is plenty of evidence of method-driven papers in Ocean Sciences (e.g. Saltzman et.al 2009, Hemming et.al 2017, Schneider-Zapp et.al 2014 and Arévalo-Martínez et.al 2013). A more detailed description of scientific results based on 4 cruises and a seasonal study is planned as a later publication, which will include discussions on the temperature/ $\text{CO}_2$  relationship and global fluxes. However, we agree that some of the results presented here can be discussed in more detail. To demonstrate how NSOP profiles may influence air/sea fluxes we have calculated how the fluxes change using the near-surface concentrations. We have added the following paragraph:

*We have adjusted the second paragraph of our conclusions (P20, L17):*

'Near surface stratification in the upper few metres of the ocean due to temperature and salinity gradients is a well-documented phenomenon. The presence or absence of chemical and biological gradients within near surface stratified layers has been difficult to assess. NSOP is a platform with the capability to successfully resolve gradients in these near surface layers. The data presented in this paper demonstrate that near surface gradients in trace gases can lead to substantially different fluxes depending upon the seawater depth that is used to calculate the flux. Assuming that the effect of temperature and salinity gradients on the flux can be accounted for using remote sensing methods (e.g. Shutler et.al 2016), then the change in flux is directly proportional to the change in  $\Delta\text{C}$ . In the case of the coastal DMS profile, a higher concentration ( $2.58 \pm 0.02 \text{ nM}$ ) was observed 0.5 m below the sea surface compared to concentrations at 5 m ( $2.36 \pm 0.03 \text{ nM}$ ). Assuming that the atmospheric concentration of DMS was negligible (a typical approach for DMS fluxes, see Lana et al., 2011), computing the flux with the 5 m waterside concentration instead of the 0.5 m waterside concentration means the flux is underestimated by 9.3%. In the case of the Celtic Sea  $\text{CO}_2$  profile, the concentration at 0.5 m ( $389.60 \pm 0.36 \mu\text{atm}$ ) was higher than at 5 m ( $385.92 \pm 0.36 \mu\text{atm}$ ). The atmospheric  $\text{CO}_2$  concentration was  $398.1 \pm 0.3 \mu\text{atm}$ , which means that the surface water was less undersaturated than implied by the seawater concentration at 5 m. Using the 5 m waterside  $\text{CO}_2$  concentration leads to an overestimation of the  $\Delta\text{C}$  and flux by 43.5% compared to using the 0.5 m waterside  $\text{CO}_2$  concentration. The magnitudes of these concentration gradients are significant.

However, such gradients (in magnitude and direction) do not persist for all hours of the day, under different environmental conditions and in all regions of the global ocean. A subsequent publication will discuss NSOP data collected during four cruises as well as the wider prevalence and implications of near surface CO<sub>2</sub> gradients.'

**Maria Ribas Ribas – Reviewer 1**

General comments

*The present paper under review for Ocean Science describes state-of-the-art technology to measure high resolution profile in the upper 5 m of the ocean. I appreciate the effort of research, develop and validation of the authors. Everyone working on R&D knows that behind these two examples profiles are a lot of trial-error and frustration. I also think the described technology fill a gap and it is really important and that it is adequate to the scope of the journal. I will recommend publication after some minor/moderate revision. I hope the comments help to improve the ms. I understand first author is PhD student and I congratulate him for the nice work .*

Specific comments

Page 4-line 15 Define ID-

As this is the only occurrence of ID, we have changed ID to inner diameter

*4-25 I am curious to know what the maximum wave height is and wind you deploy. Also applicable for my first comments on real live application.*

This information is already in the text on Pg 5 L 21-23

*5-4 What is the maximum distance?*

In this case the maximum extended length of the crane arm was ~7m. Pg 5 L 3-4 changed to

“through a block on a fully extended crane arm of 7m to maintain this distance between NSOP and the ship.”

*5-12 unfortunately I can't access to supplement material. I would love to see the videos*

*5-22 What is the limitation of the deployment length? Battery? Can other deployments, ship operations happen at the same time, like CTD, so you have a concurrence profiles?*

The information on the maximum deployment length is already in the manuscript on Pg 6 L 12-15.

The fact that no other instrumentation can be deployed simultaneously is a pertinent point. Pg 4 L 28 changed to “NSOP was always deployed while the ship was on station and not at the same time as other overboard deployments.”

*6-10 Please check figure order of appearance, suddenly here we found Fig. 9.*

1 Reference has been removed and a reference to this part of the text has been included in the caption  
2 of figure 9.

3 *7-21 In text and figure, unify use of litre with capital L*

4 All instances have been changed .

5 *7-29 How was the pressure inside the equilibrator measured?*

6 All pressure measurements were made with the Licor analyser, in close proximity to the equilibrator.  
7 Unfortunately there is no way to measure the pressure internally without compromising the  
8 membrane. We are confident that the equilibrator pressure is 0.4 kpa above ambient. Changed p7 L  
9 26 to 'The continuous gas flow through the system caused a small 0.4 kPa pressure increase in the  
10 Licor measurement cell, this was in good agreement with a similar observation by Burke Hales  
11 (0.5kpa > ambient pressure; Personal communication).'

12 *9-1:4 Could you provide more details of the membrane ( $\mu\text{m}...$ ) –*

13 The membrane material, total surface area and internal liquid and gas side volumes are now  
14 included. Pg 9 L 1 change to "We used a polypropylene membrane equilibrator (Liqui-Cel, model  
15 2.5x8) with liquid and gas volumes of 0.4 L and 0.15 L and a surface area of 1.4 m<sup>2</sup>. Due to its large  
16 surface area to volume ratio and membrane porosity (50%), the Liqui-Cel expedites gas transfer and  
17 efficiently achieves equilibration"

18 *Figure 3 caption: Could you add legend (nice to understand the figure without the need to read first).  
19 What is LPM in the x-axis?-*

20 Legends are discouraged by the ocean science journal. LPM has been changed to L min<sup>-1</sup> and ml  
21 changed to mL throughout.

22 *10-16 what is m/z –*

23 Mass is now defined as m and charge as z.

24 *10-19: two points in the reference 11-12: wrong use of () in the reference –*

25 This has been corrected.

26 *Figure 4: what is the magnitude of the change? For example from 400 to 1000 ppm or 400 to 450  
27 ppm (that will make a different, right?)? –*

28 The change was from 350 to 400 ppm for CO<sub>2</sub> and 0 to 2 nmol L<sup>-1</sup> for DMS. The absolute magnitude of  
29 the change does not matter for the calculation of response time so long as the change is large  
30 enough to be clearly detected by the instrument.

31 *I miss a table of comparison of discrete and continuous operation. Also another one of the sensor use  
32 with the accuracy/frequencies... to have a quick overlook of the system. –*

33 The two modes of deployment are not directly comparable and there is insufficient information to  
34 justify a table.

1 12-23 Probably not need to say the SOP# -

2 We feel it is helpful to retain the reference to the SOP as the document is ~200 pages.

3 In all figures, A), B) C) in the figures are capital but in the captions are not. Please unify.

4 The capitalisation in the figures has been changed.

5 14-13 How much of the unsaturated?

6 The atmospheric CO<sub>2</sub> concentration is now included. P14 L 13 changed to 'Seawater temperature was  
 7 16.61± 0.06 °C. At 14:20 hrs (UTC) fCO<sub>2(atm)</sub> was 398 µatm and fCO<sub>2(sw)</sub> was 389 µatm at 0.67 m  
 8 meaning the ocean was undersaturated with respect to the atmosphere. The temperature and  
 9 seawater CO<sub>2</sub> were the expected magnitude for summer in the Celtic Sea (Frankignoulle and Borges,  
 10 2001).'

11 15-15 Could you provide a bit more detail about this mooring? Maybe a map with location site and  
 12 the mooring will be helpful for readers not familiar with the area.

13 A map of both deployment sites is now in the supplement. Additional information about the mooring  
 14 can be found in the cruise report  
 15 [https://www.bodc.ac.uk/resources/inventories/cruise\\_inventory/reports/dy033.pdf](https://www.bodc.ac.uk/resources/inventories/cruise_inventory/reports/dy033.pdf). P15 L15  
 16 changed to 'We compare the NSOP temperature profile with thermistor readings from a series of  
 17 Sea-Bird Scientific (SBE 56) sensors (0.3, 0.6, 1.5, 3.5 and 7 m depth) mounted on a nearby  
 18 temperature chain moored ~2.8 km away (49.403°N, -8.606°E) from the deployment site'.

19 Figure 6 and 9 are quite confusing, as depth is plot with time instead as usual oceanography profile  
 20 way. In a related note, what is the different info from figure 9 and 10?

21 These plots demonstrate that the data is collected continuously at high frequency rather than  
 22 discrete samples. We have shown the time series data here as high frequency seawater pCO<sub>2</sub> data is  
 23 rarely presented, so showing how this varies is important. In addition, this paper focuses on a new  
 24 method and we want to be absolutely clear of the data processing steps that are required rather  
 25 than 'rush to the final plot'.

26 16-1:6 Can the drifting from ship cause turbulence/mixing? Would be possible to measure turbulence  
 27 within the NSOP?

28 NSOP may create a small amount of local turbulence but we did not see any evidence of this in our  
 29 profiles. It would be possible to measure turbulence from NSOP and we have added turbulence  
 30 sensors to the list of possible additional sensors on P 19 L 9.

31 17-2 When you talk about significantly different I expect a statistical test.

32 As the errors on the CO<sub>2</sub> measured by NSOP and the underway system are two standard errors, the  
 33 fact they don't overlap indicates they are statistically different at the 95% confidence interval. To be  
 34 absolutely clear, P17 L2 has been changed to 'A paired t-test showed that the fCO<sub>2</sub> measured in the  
 35 surface bins on the downcast and upcast are were significantly different (p = <0.001) .'

17-1:5 This paragraph is really important and key message of paper so I will like to have more discussion on it. What is the role of sea surface microlayer?

The sea surface microlayer was not discussed in detail as it could not be sampled with NSOP, we agree that it should be mentioned. P 17 L1 Added 'Trace gas concentrations may also be different in the sea surface microlayer but sampling that close to the surface is beyond the capabilities of NSOP. Complimentary measurements of the sea surface microlayer could be made using other state of the art purpose built sampling platforms such as the Sea Surface Scanner (Ribas –Ribas et.al., 2017).'

What is the implication of the calculations of flux as normally do it from 5 m? ...

Refer to our response to anonymous reviewer 3.

17-18:19 This comparison with underway CO<sub>2</sub> is also really important. Can you provide more detail? I will think that ship disturbance will have more influence of underway system... What is RMS? Why we should care about NSOP if they give similar results of usual pCO<sub>2</sub> instrument? I really think it is important, do not take me wrong, I just think a bit more discussion will be good

The original manuscript was unclear so we have improved the wording:

We have changed P17 L 18 to:- 'However during a deployment on the 19<sup>th</sup> July 2015, the fCO<sub>2(sw)</sub> measured by NSOP at 5 m agreed well with independent measurements from the underway system, difference = 1.7+/- 4.18 µatm, ). The agreement between the two systems is in line with previous intercomparisons (Kortzinger 2000; Ribas-Ribas 2014).

## **Anonymous – reviewer 2**

### ***General comments***

The authors presented a new sampling technique to sample and measure the vertical profiles of physical and chemical parameters in the subsurface layer of the ocean (<10 m). This indeed improves the very surface layer sampling for chemical tracers. The paper is overall well written with the exception of a few confusing sentences. Some of the figures present redundant information, and could be removed. However, the main problem of the paper, I feel, is lack of discussion on how the whole technique may impact the estimation of air-sea exchange. Does it really matter that we need to sample the very subsurface layer (e.g., ~1m) of the seawater to obtain a very accurate flux estimate? Or it may be good enough to sample 4m below the sea surface as the traditional sampling system?

In response to a similar comment from Reviewer 3, we have added a paragraph on this subject.

### ***Specific comments***

Pg2, lines 22 – 30: Authors discussed near surface stratification due to certain physical processes here. It is worth to note and mention that, people have been using CFC-11 to correct physical effect on estimated air-sea fluxes (see Lobert et al., 1995; Butler et al., 2016; Yvon-lewis et al., 2004; Hu et al., 2013).

1 This section discusses the calculation of air/sea flux using estimates of gas transfer velocity combined  
2 with global databases of trace gas concentrations. This approach to calculating air/sea flux is  
3 commonly-used in Earth System models. Near surface gradients may impact upon the calculation of  
4 air/sea fluxes.

5 We are not claiming that other approaches (such as the use of CFCs, which incorporate the implicit  
6 effects of physical forcing on gas exchange) would be influenced by near surface gradients. However,  
7 discussing the CFC method would be a deviation from the narrative of the text so we have not added  
8 anything to this effect.

9 *Pg12, lines 7 – 9: "The delay between a bucket switch and CO2 change in the Licor was timed at*  
10 *138s...". This is confusing. Does this delay include CO2 response time in the equilibrator and the time*  
11 *from sampling to the equilibrator? If it is, define it. Also, this sentence seems out of place here.*

12 P12 L7 We have changed the wording and structure of this section to improve clarity:

13 'We used different approaches to assess the delay between instantaneous miniCTD measurements  
14 and water arriving to the ship for analysis. The delay between seawater entering the inlet and  
15 reaching the equilibrator was calculated as 114 s using the internal volume of NSOP tubing (0.5 in ID,  
16 54 m length) and a seawater flow rate of 4.15 L min<sup>-1</sup>. Delay correlation analysis between the NSOP  
17 miniCTD temperature sensor and a second sensor positioned at the entrance to the equilibrator gives  
18 a similar delay of 112 s. Note that the total delay of the system is greater because it also includes the  
19 time that equilibrated gas takes to reach the Licor. We determined the total delay by moving the  
20 seawater inlet quickly between two buckets with distinctly different CO<sub>2</sub> concentrations and timing  
21 how long it took for the signal to be detected by the Licor (139 s; Fig. 4).'

22

23 *Pg12, lines 21 – 25: list equations to be clearer.*

24 The equations are commonly used by the community and are well detailed in (Dickson 2007). We  
25 feel this is sufficient.

26 *Pg 12, lines 26 – 28: redundant information.*

27 Removed

28 *Fig. 5: I don't think this figure provides extra information or value other than the sentence described*  
29 *in Pg 11, line 21. So, you may consider remove it.*

30 The reference to this figure remains in the text but the figure has now been moved to the  
31 supplement.

32 *Figs. 6 & 7: Redundant. Recommend to remove fig. 6. Figs. 9 and 10: redundant information.*  
33 *Consider remove fig. 9*

1 Please see earlier response to Ribas-Ribas.

2 *Also, fig. 7 looks a little messy with depth contours.*

3 The lines in Fig. 7c are not depth contours. They are a time series of temperature for sensors at  
 4 different depths. We have added additional detail to the figure legend to clarify this.

5 *Pg. 16, line 18: Density was not used in the later discussion. I am not sure why you want to mention*  
 6 *and discuss density profiles here. Consider remove it from the text and figure.*

7 Density determines the stratification and is affected by both salinity and temperature. We think it is  
 8 necessary to include density as it is more useful to the reader than just plotting temperature.

9 *Pg. 17, lines 3 – 5: why do fco2 profiles show the largest difference in the surface, and not in the layer*  
 10 *where the temperature showed the largest difference (4.5 – 2 m below water)? The explanation given*  
 11 *by the authors is not convincing. Since the amount of co2 outgassing due to surface seawater*  
 12 *warming (during upcast) can be calculated using temperature, salinity and solution of CO2, it is not*  
 13 *hard to estimate how much the difference between down cast and up cast was due to physical effect,*  
 14 *and how much was due to biological influences.*

15 We are a bit confused by this comment. Figure 8 shows that there is a gradient in fCO<sub>2</sub> down to a  
 16 depth of 5 m. The temperature effect on fCO<sub>2</sub> is already accounted for - the profile we show is  
 17 seawater fCO<sub>2</sub> after correction for *in situ* temperature.

18 *Pg. 17, lines17–19: 3 uatm seems ahuge difference considering the variation off co2 observed in the*  
 19 *subsurface layer. Did the authors consider the different response time in two different equilibrators?*  
 20 *Why are their measured values so different?*

21 We apologise - our original text is misleading. We said that “CO<sub>2</sub> agrees to within 3 uatm” but the  
 22 mean difference is actually 1.7+/- 4.18 uatm. This is very similar to previous comparisons between  
 23 shower and membrane equilibrators (Hales et.al., 2004). This is also close to the (Kortzinger et.al.,  
 24 2000) comparison of 1 uatm, which used very similar equilibrator setups. As detailed in our response  
 25 to reviewer Ribas-Ribas, we have changed the paragraph on P17, L 17-19 to make this clearer. Also,  
 26 note that we do consider the response time in the equilibrators (see text on P10, L1-14).

27 *Pg. 18, lines 15 – 16: confusing. To me, the increased fluorescence is likely due to phytoplankton*  
 28 *located at the bottom or below the subsurface layer. –*

29 We disagree. It is well established that phytoplankton fluorescence becomes quenched in the very  
 30 near surface layers and does not suggest a change in phytoplankton concentration with depth. (Serra  
 31 et.al 2007, Gibb et.al 2000 and Smyth et.al 2004).



# A measurement system for vertical seawater profiles close to the air/sea interface

Richard P. Sims<sup>1,2</sup>, Ute. Schuster<sup>2</sup>, Andrew. J. Watson<sup>2</sup>, Ming Xi. Yang<sup>1</sup>, Frances. E. Hopkins<sup>1</sup>, John. Stephens<sup>1</sup> and Thomas. G. Bell<sup>1,\*</sup>

[1]{Plymouth Marine Laboratory, Plymouth, United Kingdom}

[2]{University of Exeter, Exeter, United Kingdom}

*Correspondence to:* T. Bell (tbe@pml.ac.uk)

## Abstract

This paper describes a Near Surface Ocean Profiler, which has been designed to precisely measure vertical gradients in the top 10 m of the ocean. Variations in the depth of seawater collection are minimised when using the profiler compared to conventional CTD/rosette deployments. The profiler consists of a remotely operated winch mounted on a tethered yet free floating buoy, which is used to raise and lower a small frame housing sensors and inlet tubing. Seawater at the inlet depth is pumped back to the ship for analysis. The profiler can be used to make continuous vertical profiles or to target a series of discrete depths. The profiler has been successfully deployed during wind speeds up to  $10 \text{ m s}^{-1}$  and significant wave heights up to 2 m. We demonstrate the potential of the profiler by presenting measured vertical profiles of the trace gases carbon dioxide and dimethylsulfide. Trace gas measurements use an efficient microporous membrane equilibrator to minimise the system response time. The example profiles show vertical gradients in the upper 5 m for temperature, carbon dioxide and dimethylsulfide of  $0.15 \text{ }^{\circ}\text{C}$ ,  $4 \text{ } \mu\text{atm}$  and  $0.4 \text{ nM}$  respectively.

## 1 Introduction

Exchange between the ocean and atmosphere is an important process for many gases. Important examples include carbon dioxide ( $\text{CO}_2$ ), for which the oceans account for 25% of the sink for anthropogenic emissions (Le Quéré et al., 2016), and dimethylsulfide (DMS),

1 which has an oceanic source and influences cloud properties with implications for the global  
2 energy balance (Quinn and Bates, 2011). The magnitude and direction of air/sea gas transfer  
3 is typically represented by  $\text{Flux} = K\Delta C$  (Liss and Slater, 1974), where  $\Delta C$  is the concentration  
4 difference across the air-sea interface and  $K$  is the gas transfer velocity. Direct flux  
5 measurements (Bell et al., 2013; Yang et al., 2013; Miller et al., 2010) are only possible for a  
6 small number of gases and are not made routinely. Most flux estimates use a wind speed-  
7 based parameterisation of  $K$  (e.g. Wanninkhof, 2014) coupled with measurements of  $\Delta C$ .

8  $\text{CO}_2$  is the most well-observed trace gas in the surface ocean, with 14.5 million measurements  
9 compiled into a global database, the Surface Ocean  $\text{CO}_2$  Atlas (SOCAT),  
10 <http://www.socat.info/> (Bakker et al., 2016). Global trace gas databases also exist for gases  
11 such as methane and nitrous oxide <https://memento.geomar.de/> (Bange et al., 2009),  
12 dimethylsulfide <http://saga.pmel.noaa.gov/dms/> (Lana et al., 2011) and halocarbons  
13 <https://halocat.geomar.de/> (Ziska et al., 2013). Accurate estimation of air/sea flux requires  
14 concentration measurements that are representative of the interfacial concentration difference.  
15 Surface seawater samples are often collected from the underway seawater intake of research  
16 vessels, typically at 5-7 m depth. A source of potential error in air/sea flux calculations arises  
17 from the assumption of vertical homogeneity within the mixed layer (Robertson and Watson,  
18 1992). If vertical concentration gradients exist in the mixed layer, then underway seawater is  
19 not representative of the interfacial layer, which could create a global sampling bias (McNeil  
20 and Merlivat, 1996).

21 Vertical gradients in trace gas concentrations have been observed under conditions that are  
22 favourable for near surface stratification (Royer et al., 2016). At low wind speeds, high solar  
23 irradiance can suppress the depth of shear-induced mixing to create a near surface layer  
24 several degrees warmer than the water below (Ward et al., 2004; Fairall et al., 1996). Near  
25 surface stratification in the marine environment can also be induced by freshwater inputs such  
26 as rain (Turk et al., 2010) and riverine discharge. Changes in surface seawater temperature  
27 and salinity alter the solubility of dissolved gases and thus the amount available for air/sea  
28 exchange (Woolf et al., 2016). Dissolved gases isolated in the upper few metres of the ocean  
29 may additionally be modified by physical process such as air/sea exchange and  
30 photochemistry. Marine biota confined within the stratified layer (Durham et al., 2009), may  
31 also alter trace gas concentrations. For the purposes of this paper, near surface gradients are  
32 defined as physical and/or chemical gradients in the upper 10 m of the ocean.

Identifying and quantifying near surface gradients in trace gas concentrations is challenging. Ship motion often inhibits near surface measurements made with the standard oceanographic approach of sampling with Niskin bottles mounted on a CTD rosette. Substantial vertical movement of the rosette limits how close to the surface a sample can be taken. For example, a crane arm 4 m above the sea surface and 11 m from the centreline of a ship that is rolling by  $\pm 4$  degrees will induce  $\sim 1.5$  m sample depth variation every few seconds. CTD/Niskin bottle sampling requires that the rosette is kept below the sea surface. Sampling within 2 m of the sea surface is often impossible, even under relatively calm conditions.

We present a Near Surface Ocean Profiling buoy (NSOP) designed for measuring near surface profiles. The design principles for NSOP were:

- (1) Platform diameter less than the wavelength of most open ocean waves, allowing it to ride the swell;
- (2) Short sampling arm close to the sea surface to reduce vertical movements induced by platform motion;
- (3) Capable of deployment close to the ship (to retrieve water for trace gas analysis), but away from major turbulence and motion due to the ship itself.

Example profiles from a cruise on the European continental shelf (*RRS Discovery*, DY033, July 2015) and in the English Channel on board the *RV Plymouth Quest* (part of the Western Channel Observatory, Smyth et al., 2010, April 2014) are discussed.

## 2 Methods

### 2.1 Near Surface Ocean Profiler (NSOP) description

NSOP is a repurposed ocean buoy (1.6 m diameter) with a central lifting eyelet (Fig. 1). The top of the buoy is 0.5 m above the sea surface. Mounted on top of the buoy are a line of sight, remotely operated winch (Warrior Winch, model C8000) and a gel battery (Haze, model HZY-S112-230). The winch feeds Kevlar rope through a block and tackle with a 3:1 ratio to reduce rope pay-out speed to  $\sim 0.05 \text{ m s}^{-1}$ . The block and tackle is attached to the end of an outstretched arm 0.25 m from the outer edge of the buoy. The winch line is attached to an open frame (0.35 m diameter, 0.8 m height) with the capacity to house multiple sensors. Desired sampling depth is targeted using knowledge of the winch pay-out speed. Rope pay-

out is then timed with a stopwatch. This approach only approximately regulates the sampling depth because: (i) winch pay-out varies slightly depending on the amount of rope on the spool; and (ii) variable horizontal current strength affects the vertical versus horizontal position of the sampling frame. To minimise horizontal movement of the sampling frame we attached a 10 kg weight to the base of the frame.

The primary sensor on the sampling frame is a small CTD (Valeport miniCTD) set to sample at a high frequency ( $>1$  Hz). Under calm conditions it is possible to sample as close as 0.1 m from the air/sea interface when the miniCTD and tubing are mounted near the top of the frame. Rougher conditions demand that the frame be kept deeper ( $\sim 0.5$  m) as motion can momentarily bring the sensors and tubing out of the water. An emergency tag line was attached to the sampling frame in case the winch line failed. Seawater for trace gas analysis was pumped back to the ship at  $3.5 \text{ L min}^{-1}$  through a 50 m PVC hose (0.5 in ~~inner~~ diameter). A heavy duty peristaltic pump (Watson Marlow, model 701IB/R), primed with water from the ship's underway supply was used to overcome the large hydraulic head ( $\sim 4$  m). The open end of the tubing was located at the same depth as the miniCTD. Water arriving to the ship's laboratory was divided, with  $\sim 3.0 \text{ L min}^{-1}$  for flow-through analysis (e.g. equilibrator for trace gases) and  $\sim 0.5 \text{ L min}^{-1}$  for discrete samples (e.g. total alkalinity).

We assessed the depth resolution capability of NSOP at a particular depth by looking at pressure variations under calm conditions with a fixed amount of winch rope paid out. In calm to moderate conditions ( $<2.5$  m significant wave height) the amount of vertical movement indicated by the standard deviation (SD) in the depth is  $\pm 0.18$  m (see Fig. S2-S1 in ~~Supplemental-supplementary~~ information). During 4 deployments in rough conditions ( $>2.5$  m significant wave height), the depth variability increased as the sampling frame was lowered (at 5 m, SD was  $\pm 0.275$  m).

## 2.2 NSOP deployment

On a large research vessel such as the *RRS Discovery*, the deployment and recovery of NSOP requires close coordination between the bridge and 3 personnel on deck. NSOP was always deployed while the ship was on station and not at the same time as other overboard deployments. Ship orientation during deployments was typically with bow into the wind but also accounted for swell and current direction/speed. NSOP was lifted by the aft crane (Fig. 1). Once NSOP was lowered to the surface it was detached from the crane via a quick release.

Two slack lines were looped through eyelets on the free-floating NSOP to maintain its position close to the ship. A third slack line was connected to the top of the buoy and passed through a block on a fully extended crane arm ~~to maintain distance (minimum 7 m)~~ of 7 m to maintain this distance between NSOP and the ship. The slack lines successfully inhibited the tendency of NSOP to drift horizontally without disrupting its ability to ride the swell. The instrument frame acted like a sea anchor and minimised rotation of NSOP. A 4 m lifting strop used for recovery was connected to the lifting eyelet and loosely lashed to the aft slack line. During retrieval, the slack lines were hauled in and the crane and jib arms brought towards the ship to bring NSOP alongside. The lifting strop was then parted from the slack line and attached to the crane to lift NSOP back on deck. For additional photographs of a NSOP deployment and videos of NSOP during a deployment and in operation, see Fig. S2 and videos, supplemental material ~~ry~~ information.

Turbulence from the ship's propellers has the potential to mix the water column and destroy any near surface gradients. The ship did not use the aft thrusters whenever conditions were suitable (mild sea state, weak currents and no local hazards). Keeping NSOP away from the ship limited disruption of near surface gradients by the thrusters and reduced the risk of line entanglement in the aft propellers. Our winch did not have a groove bar to feed the rope onto the winch drum, leading to an increased likelihood of snagging during spooling. To minimize snagging, the rope was manually fed onto the winch spool before deployments. Visual monitoring of the NSOP frame, slack lines and winch spool is important during deployment.

NSOP has been successfully deployed in 'moderate' sea states up to Beaufort force 5 (~10 m s<sup>-1</sup> wind speed and wave heights of ~2.0 m). Deployment length typically varied from 1-3 hours.

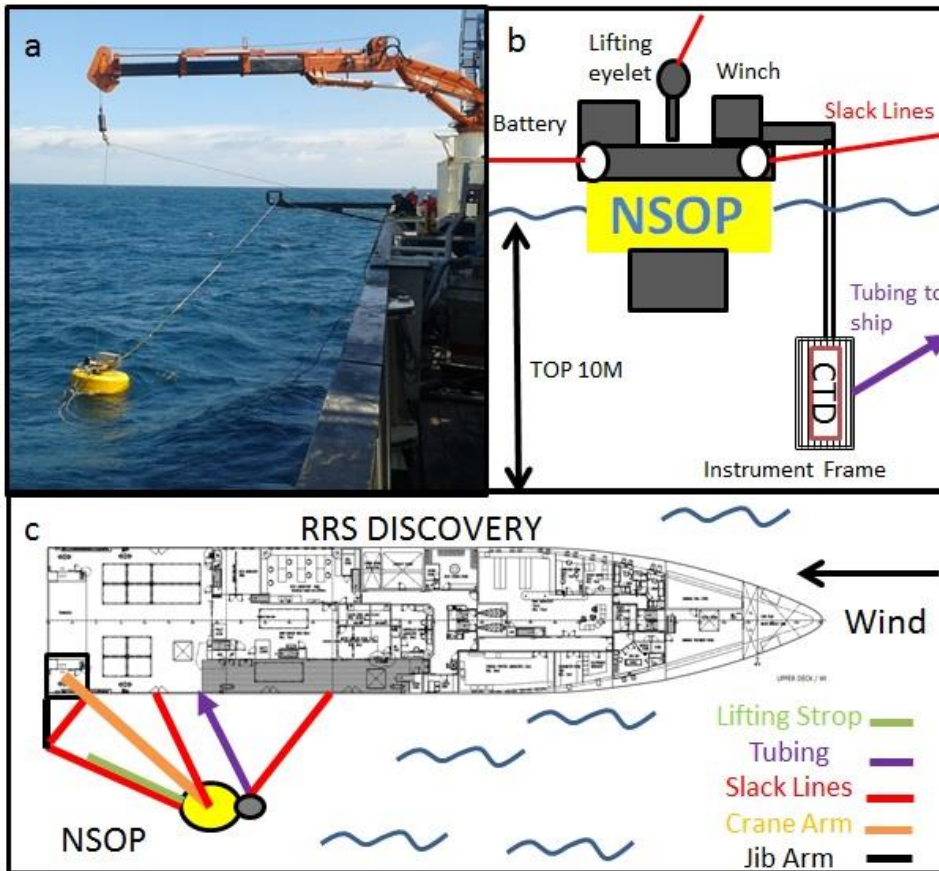


**Figure 1:** Different points of view of an NSOP deployment: (a) Image from a deployment on *RRS Discovery* in May 2015 (Cruise DY030); (b) Schematic cross section of NSOP including tubing back to ship (purple) and slack lines (red); and (c) Top down schematic from a research ship including ship orientation. Not to scale.

NSOP can be used in two profiling modes: ‘continuous’ and ‘discrete’. Continuous profiling maximises vertical coverage and involves the winch continuously paying rope in and out at  $\sim 0.05 \text{ m s}^{-1}$ . A complete down/up profile to 10 m can be conducted in approximately 7 min (Fig. 9). Depth resolution during continuous profiling is determined by the measurement response time. Instruments with rapid response times such as the miniCTD temperature and conductivity sensors (0.15 s and 0.09 s) have theoretical depth resolutions of 0.75 cm and 0.45 cm respectively. Actual depth resolution will also be affected by the sampling depth variability of the NSOP instrument frame. A measurement setup with a longer response time (such as for seawater  $\text{CO}_2$ ) requires a different approach (see Section 2.5).

During discrete profiling, the winch pays out a fixed amount of rope (typically 0.5 m) and the sampling frame is left at a fixed depth. After a fixed sampling period, more rope is paid out. The process is repeated down and then up such that a set of discrete depths are sampled in a 'stepped' profile. The discrete profiling depth resolution is determined by the depth fluctuations when sampling at a fixed depth (see Section 2.1). Discrete profiles are a more appropriate approach for measurement systems with a longer response time. A discrete profile with 0.5 m steps down to 5 m and back to the surface using a 2.5 min sampling period takes about an hour. The sampling period at each depth and frequency/distribution of depths within the profile can be adjusted to suit sampling priorities.

The maximum deployment time is limited by the capacity of the winch battery. When under no load, the battery allows for approximately 3 hours of operation in the continuous mode. Discrete profiling requires substantially less winch usage such that battery drainage is even less of a concern.

### 2.3 CO<sub>2</sub> analysis

The CO<sub>2</sub> measurement system (Fig. 2) is a modified version of the system described by (Hales et al., 2004). Seawater from the NSOP inlet was passed through the equilibrator (see Section 2.3.1) at  $\sim 3 \text{ L min}^{-1}$  and the flow rate monitored (Cynergy ultrasonic flow meter, model UF25B). A compressed nitrogen gas supply, maintained at a constant flow rate of 100 ~~mL~~ mL  $\text{min}^{-1}$  (Bronkhurst mass flow controller, model F-201-CV-100) flows through the equilibrator in the opposite direction to the seawater flow. The gas has high water vapour content after equilibration and is dried (Permapure nafion dryer, model MD-110-48S-4). The dried sample then enters the analytical cell of a NDIR Licor 7000, which is protected with a 0.2  $\mu\text{m}$  filter (Pall, Acro 50).

CO<sub>2</sub> measurements at atmospheric pressure as recommended by Dickson et al. (2007) were not possible due to the nature of the experimental setup. The continuous gas flow through the system caused a small 0.4 kPa pressure increase in the Licor measurement cell, this was in good agreement with a similar observation by Burke Hales (0.5kpa > ambient pressure; Personal communication). The elevated pressure was taken to be representative of the equilibrator pressure and was used to obtain the partial pressure of CO<sub>2</sub> in the equilibrator ( $p\text{CO}_{2(\text{eq})}$ ).

The Licor was calibrated using three CO<sub>2</sub> standard gases before and after each NSOP deployment. The concentrations of the standard gases (BOC Ltd.) were determined by referencing against US National Oceanic and Atmospheric Administration certified standards (244.91, 388.62, 444.40 ppm) in the laboratory. The seawater temperature at the entry and exit ports of the equilibrator was recorded at 1 Hz (Omega ultra-precise 1/10 DIN immersion RTD) using stackable microcontrollers (Tinkerforge master brick 2.1 and PTC bricklet). Equilibrator temperature probes and the miniCTD temperature sensor were calibrated before and after each cruise against an accurate reference sensor (Fluke, model 5616-12,  $\pm 0.011^{\circ}\text{C}$ ) in a stable water bath (Fluke 7321).

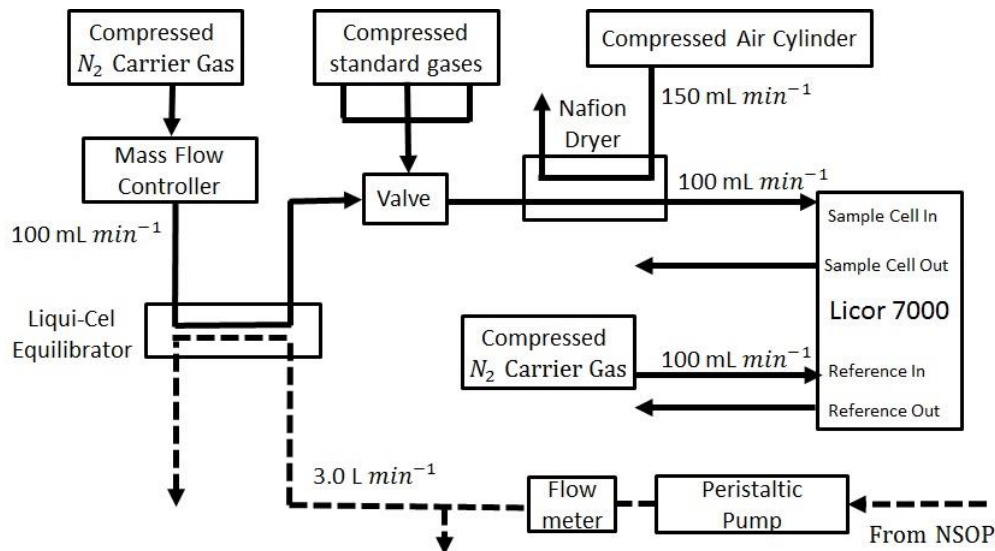


**Figure 2:** CO<sub>2</sub> system schematic. Solid and dashed arrows correspond to gas and water flows respectively. The Licor reference cell is flushed with equilibrated gas at 100 ~~mL~~ mL min<sup>-1</sup>. A manual selection valve was used to switch between equilibrated gas and the CO<sub>2</sub> standards.

### 2.3.1 Equilibrator

The showerhead equilibrator is the most commonly-used equilibrator for CO<sub>2</sub> but takes ~100 s to equilibrate (Dickson et al., 2007; Kitidis et al., 2012; Körtzinger et al., 2000; Webb et al., 2016). This equilibration time is too slow for effective use during NSOP deployments. We used a polypropylene membrane equilibrator (Liqui-Cel, model 2.5x8) with liquid and gas



volumes of 0.4 L and 0.15 L and a surface area of 1.4 m<sup>2</sup>. ~~because Due to it has a~~ large surface area to volume ratio and membrane porosity (50%). ~~t.~~ The Liqui-Cel expedites gas transfer and efficiently achieves equilibration (Loose et al., 2009), with a 3 s response time for CO<sub>2</sub> (Hales et al., 2004). Membrane equilibrators have been used by others for trace gas analysis (Hales et al., 2004; Marandino et al., 2009).

Fugacity of seawater CO<sub>2</sub> is calculated from the Licor gas phase CO<sub>2</sub> measurement. This approach assumes that the gas phase sample has equilibrated fully with the seawater. We performed equilibration efficiency experiments in a seawater tank using a showerhead equilibrator as a reference. Liqui-Cel equilibration efficiency declined after prolonged exposure to seawater, likely due to biofouling of the membranes. In a fouled equilibrator, equilibration efficiency was a function of the flow rate on both the water and gas side of the membrane. An increased gas flow rate reduces the residence time inside the Liqui-Cel and allows less time to equilibrate (Fig. 3a). Increasing the waterside flow rate moves the gas phase closer to equilibrium because the transfer coefficient in the membrane increases (Fig. 3b).

Cleaning with an acid - base sequence restored the efficiency of a fouled equilibrator. It was necessary to actively pump chemicals through the Liqui-Cel to achieve a full recovery in efficiency. For more details on cleaning techniques, see supplemental material. Efficiency reductions in membrane equilibrators like the Liqui-Cel have not been reported by previous studies. Some authors have used 5-50 µm filters to minimise biofouling (Hales et al., 2004) (~~Hales et al., 2004~~) but this was not possible with the NSOP experimental design. If filtering seawater is not possible, we recommend flushing with freshwater after use, regular cleaning of the Liqui-Cel and daily tests to quantify equilibration efficiency. Trace gas measurement systems that use an internal liquid phase standard (e.g. dimethylsulfide, Section 2.4) account for any changes in equilibrator efficiency.

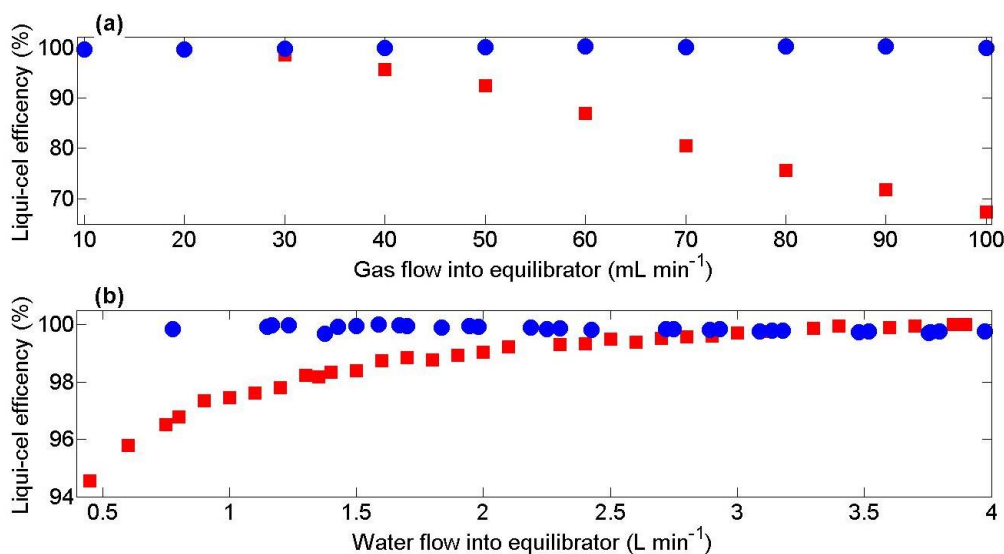


**Figure 3:** Liqui-Cel CO<sub>2</sub> equilibration efficiency (Liqui-Cel mixing ratio / showerhead mixing ratio) for: (a) changing gas flow at a fixed water flow rate of 4 L min<sup>-1</sup>; and (b) changing water flow at a fixed gas flow of 100 mL min<sup>-1</sup>. Blue = unfouled equilibrator. Red = fouled equilibrator.

## 2.4 DMS analysis

DMS was measured with Atmospheric Pressure-Chemical Ionisation Mass Spectrometry (API-CIMS), using a system modified following Saltzman et al. (2009). Measurements were calibrated using an isotopic liquid standard of tri-deuterated DMS (see Bell et al., 2013 for details) (Bell et al., 2013 for details). Isotopic standard was injected at 120  $\mu\text{L min}^{-1}$  into the 3 L min<sup>-1</sup> seawater flow from NSOP before it entered the Liqui-Cel equilibrator. Compressed nitrogen gas was passed through the equilibrator in the counter direction to the seawater flow at 1 L min<sup>-1</sup>. The use of an internal standard meant that any incomplete equilibration of the ambient non-isotopic DMS was also true for the isotope. The gas stream exited the equilibrator and was dried (Permapure nafion dryer, model MD-110-48S-4) before entering the mass spectrometer for analysis. DMS was detected at  $m/z$  (mass/charge) 63 and the isotopic standard detected at  $m/z$  66. The concentration of DMS was calculated using the ion signals and relevant flow rates (Bell et al., 2015). This approach has been shown to compare well with other analytical techniques for DMS (Royer et al., 2014; Walker et al., 2016) (Walker et al., 2016; Royer et al., 2014).

## 2.5 NSOP ~~response delay~~ and ~~response delay~~-time

We used different approaches to assess the delay between instantaneous miniCTD measurements and water arriving to the ship for analysis. The delay between seawater entering the inlet and reaching the equilibrator was calculated as 114 s using the internal volume of NSOP tubing (0.5 in inner diameter, 54 m length) and a seawater flow rate of 4.15 L min<sup>-1</sup>. Delay correlation analysis between the NSOP miniCTD temperature sensor and a second sensor positioned at the entrance to the equilibrator gives a similar delay of 112 s. Note that the total delay of the system is greater because it also includes the time that equilibrated gas takes to reach the Licor. We determined the total delay by quickly transferring the seawater inlet quickly between two buckets with distinctly different CO<sub>2</sub> concentrations and timing how long it took for the signal to be detected by the Licor (139 s; Fig. 4).

The response time of the NSOP setup was determined by simulating step changes in gas concentrations. ~~The tubing inlet was quickly transferred between two buckets of seawater with a distinct difference in concentration.~~ A model fit to the exponential change in signal was used to estimate the response time (Fig. 4). We estimate the system response time (e-folding time) for CO<sub>2</sub> as 24 s, which is slightly faster than the 34 s reported by Webb et al. (2016). The e-folding time in the DMS signal is estimated as 11 s, which is consistent with the rapid gas flow rate through the analytical system.

Continuous profiling with the CO<sub>2</sub> system and a 24 s response time yields a depth resolution of 1.2 m, which is greater than the required resolution to assess near surface gradients. DMS has a faster response time than CO<sub>2</sub>, but in continuous profiling mode this only translates to a depth resolution of 0.6 m, slightly less than the 1.2-2 m reported by (Royer et al., 2014). A depth resolution of < 0.5 m was desired to capture upper ocean vertical gradients in CO<sub>2</sub> and DMS so NSOP was operated in discrete profiling mode.

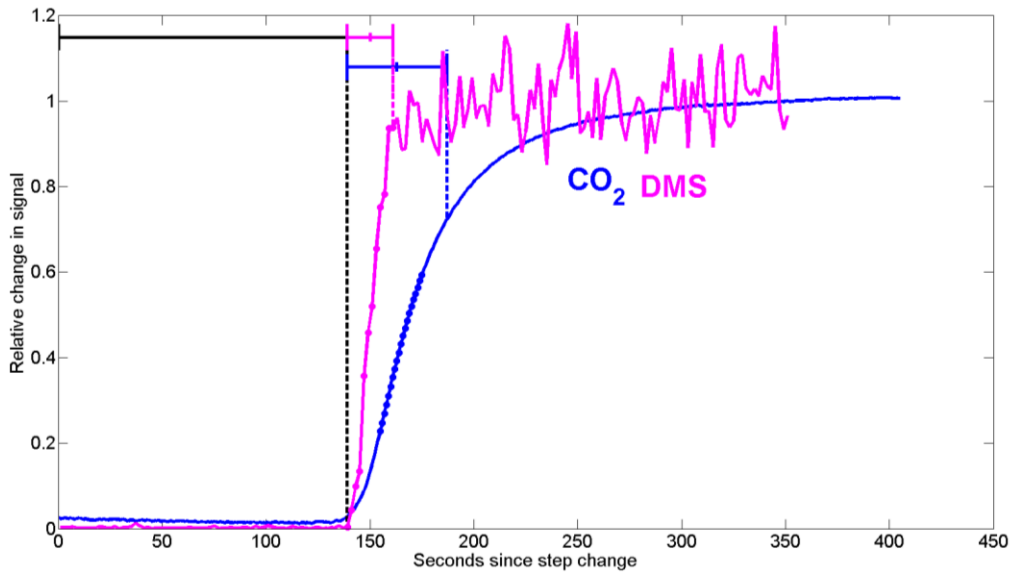


**Figure 4:** Instrument responses to step changes in seawater CO<sub>2</sub> (blue) and DMS (magenta). Step changes from 350 to 400  $\mu\text{atm}$  for CO<sub>2</sub> and 0 to 2  $\text{nmol L}^{-1}$  for DMS have been scaled down so that the initial and end concentrations are between 0 and 1. Instrument responses have been scaled so that the initial and end concentrations are between 0 and 1. Time is referenced against the point when the step change was initiated. The response is seen in both instruments after a delay of 138 s (black dashed line). Two e-foldings are indicated by vertical dashed lines for CO<sub>2</sub> (blue) and DMS (magenta). The data points marked by circles were used to make an exponential fit to the data to determine the response time (Sect 2.5).

We used different approaches to assess the delay between instantaneous miniCTD measurements and water arriving to the ship for analysis. Using the internal volume of NSOP tubing (0.5 in ID, 54 m length) and a seawater flow rate of  $4.15 \text{ L min}^{-1}$ , the tubing delay to the equilibrator was calculated as 114 s. Delay correlation analysis between the NSOP miniCTD temperature and a temperature sensor positioned at the entrance to the equilibrator suggests a delay of 112 s. The delay between a bucket switch and a CO<sub>2</sub> change in the Licor was timed at 138 s. The bucket switch delay was longer because the bucket switch experiment also accounts for the delay in the equilibrator and the Licor.

## 2.6 Data processing

During discrete profiling, distinct sample depths were identified from the rapid changes in pressure during depth transitions. Data were binned into discrete depth bins using CTD pressure measurements. Trace gas data were assigned to depth bins after adjusting for the calculated transit time through the NSOP tubing (Section 2.5). CO<sub>2</sub> data from the beginning (2 e-foldings + 15 s buffer = 63 s) and end (15 s buffer) of each depth bin was excluded from analysis to account for the response time of the system and the transition time between sample depths. The same approach was taken for DMS, where the faster response time resulted in a smaller portion of data excluded at the beginning of each depth bin (2 e-foldings + 15 s buffer = 37 s).

The CO<sub>2</sub> mixing ratio ( $x_{CO_2}$ ) measured in the Licor is converted to equilibrator fugacity ( $f_{CO_{2(eq)}}$ ) using calibration standards, *in situ* seawater salinity, and the pressure and temperature in the equilibrator (SOP 5# Underway pCO<sub>2</sub> Dickson et al., 2007). Vertical profiles of seawater CO<sub>2</sub> fugacity ( $f_{CO_{2(sw)}}$ ) are calculated using average equilibrator fugacity ( $f_{CO_{2(eq)}}$ ), equilibrator temperature ( $T_{(eq)}$ ) and *in situ* seawater temperature ( $T_{(sw)}$ ) at each depth (Takahashi et al., 1993). ~~The time series  $f_{CO_{2(sw)}}$  data shown in (Fig. 7) are also calculated using the same equation from Takahashi et al. (1993) but instead use high frequency  $f_{CO_{2(sw)}}$ ,  $T_{(eq)}$  and  $T_{(sw)}$  data.~~

## 2.7 Seawater sample collection using NSOP

The NSOP setup enables vertical profiles of discrete seawater samples to be collected from upstream of the equilibrator, with a split in the tubing diverting ~0.5 L min<sup>-1</sup> into a sink. For example, discrete seawater samples (250 ml) have been successfully collected and analysed for Total Alkalinity (TA). Samples were collected and poisoned following best practice recommendations (SOP#1, (Dickson et al., 2007). Bottle filling plus 1 overfill took ~60 s. Start and end times were recorded so that collection depth could be retrospectively determined from the CTD pressure data. Analytical methods and an example depth profile (Fig. S3) are provided in the supplementary information.

### 3 Field Measurements / Observations

Presented below are example profiles collected using NSOP. The first deployment was in the open ocean (July 30<sup>th</sup> 2015, Central Celtic Sea; 49.4213°N, -8.5783°E) from the *RRS Discovery* (100 m length, 6.5 m draught). The second deployment was in coastal waters (15<sup>th</sup> April 2014, Plymouth Sound; 50.348°N, -4.126°E) from the *RV Plymouth Quest* (20 m length, 3 m draught). [A map of deployment sites is supplied in the supplementary information.](#)

#### 3.1 Open ocean deployment

NSOP was deployed at 14:05 (UTC) on 30<sup>th</sup> July 2015. During the 6 hours preceding deployment, the ship was on station and encountered persistently strong solar radiance ( $> 600 \text{ W m}^{-2}$ ), mild winds ( $< 6 \text{ m s}^{-1}$ ) and calm sea state (significant wave height  $< 1.6 \text{ m}$ ). This combination of low wind speeds and high irradiance (Fig. [S5, supplementary information](#)) is favourable for near surface stratification (Donlon et al., 2002).

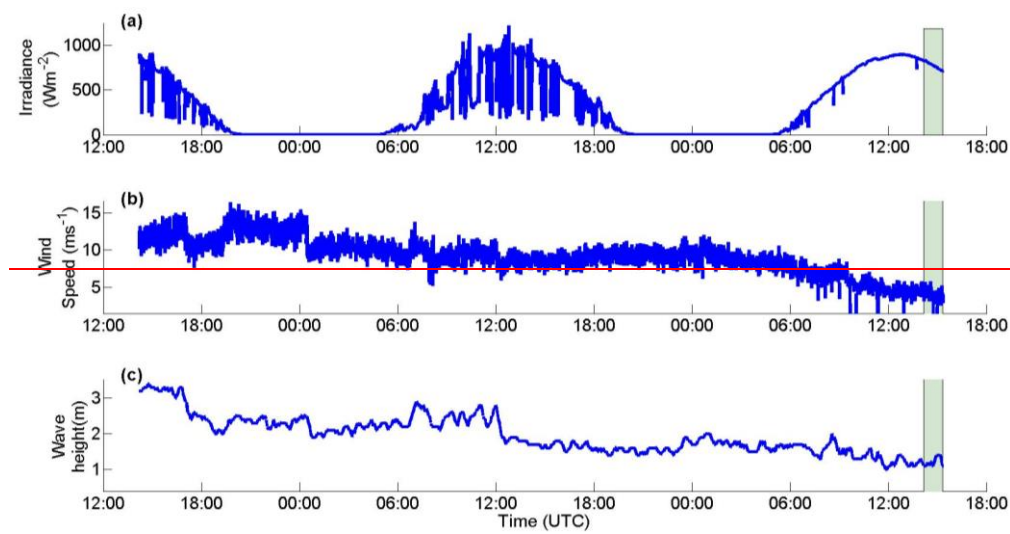


**Figure 5:** Timeseries of meteorology and sea state variables in the Celtic Sea in July 2015 while the ship was on station: (a) irradiance; (b) wind speed; and (c) significant wave height. The data begin 48 h before the start of the profile at 14:05 hrs (UTC). The vertical grey bar indicates the period when NSOP was profiling.

Fig. 6.5 presents the time series data collected by NSOP for depth, temperature, salinity and  $\text{fCO}_{2(\text{sw})}$ . Discrete profiling began at 14:05 hrs (UTC) at 0.7 m depth, which was as close to

the surface as the frame could be located without the possibility of breaking the surface. Depth bins were identified based on rapid depth transitions (Fig. 6a5a). Bottles were filled for discrete samples during the downcast. Profiling lasted 75 minutes and finished back at the surface at 15:20 hrs (UTC). Seawater temperature was  $16.61 \pm 0.06$  °C. At 14:20 hrs (UTC)  $f\text{CO}_{2(\text{atm})}$  was 398  $\mu\text{atm}$  and  $f\text{CO}_{2(\text{sw})}$  was 389  $\mu\text{atm}$  at 0.67 m. Seawater temperature was  $16.61 \pm 0.06$  °C and  $f\text{CO}_{2(\text{sw})}$  was meaning the ocean was undersaturated with respect to the atmosphere. The temperature and seawater  $\text{CO}_2$  both were the expected magnitude for summer in the Celtic Sea (Frankignoulle and Borges, 2001). Salinity was homogeneous throughout the NSOP deployment, only varying by  $\pm 0.004$ .

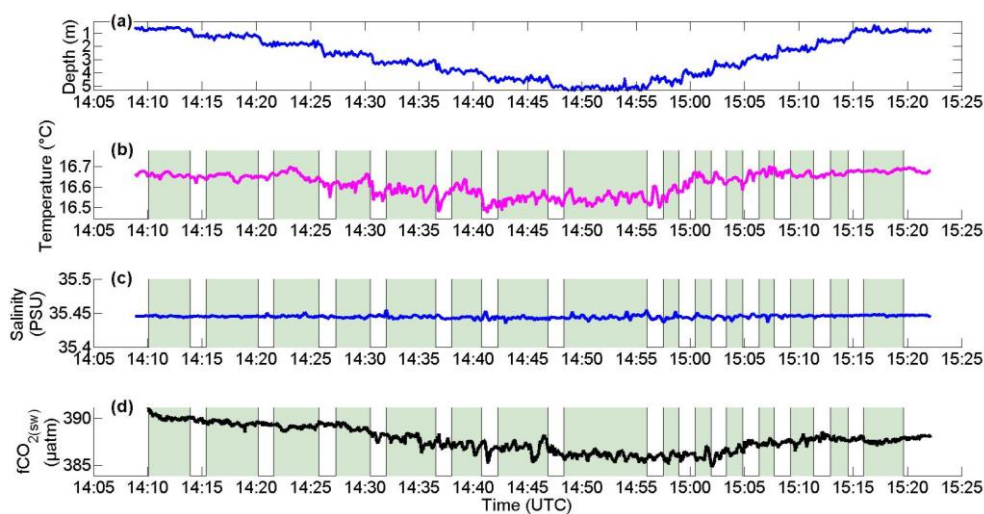


**Figure 65:** Time series measurements made during an NSOP deployment in the Celtic Sea on 30<sup>th</sup> July 2015. Data are 1 Hz depth (a), seawater temperature (b), salinity (c) and  $f\text{CO}_{2(\text{sw})}$  (d). Data used for depth bin analysis (Section 2.6) is identified by a shaded background.

Depth-binned salinity and temperature data did not show any significant variability (Fig. 7a6a). A slight temperature gradient was observed, with  $0.15$  °C difference between 5 m and the surface and a fairly constant reduction with depth ( $0.03$  °C per metre). The temperature profile was similar for down and up casts, although some continued warming of surface waters was evident in the up cast. The temperature measured by NSOP at 5.15 m depth agrees well with the coincident temperature measured by the bow thermistor at 5.5 m ( $< 0.02$  °C difference) (Fig. 7e6c). There is no evidence that the ship's thrusters/propellers disrupted the near surface gradients.

We compare the NSOP temperature profile with thermistor readings from a series of [Sea-Bird Scientific \(SBE 56\)](#) sensors ([0.3, 0.6, 1.5, 3.5 and 7 m depth](#)) mounted on a [nearby temperature chain](#) moored [~2.8 km away \(49.403°N, -8.606°E\)](#) from the deployment site ([0.3, 0.6, 1.5, 3.5 and 7 m depth](#)). The vertical profile implied by the NSOP deployment agrees with the mooring data (Fig. [7e6c](#)), and corroborates the warming of the upper few metres of the ocean observed during the deployment. The agreement between these independent datasets suggests that it is unlikely that NSOP caused any significant localized warming of surface waters. The mean difference between NSOP temperature from discrete depths and the mooring sensors is 0.02°C. The surface data from the NSOP up cast show less agreement with the mooring, with NSOP temperatures ~0.05 °C lower than the 0.3 m and 0.6 m mooring sensors. During the profile the ship drifted ~1 km from the start position of the profile and a further 0.2 km from the mooring. The small offset between the NSOP surface temperatures and the mooring may be driven by horizontal variability between the deployment and mooring locations. It is also possible that turbulence mixed warm surface waters down into cooler sub-surface layers. Turbulence could have been generated around the NSOP sampling frame or by an increase in wave-driven mixing when the significant wave height increased at ~15:00 hrs UTC (Fig. [5AS4a](#)).

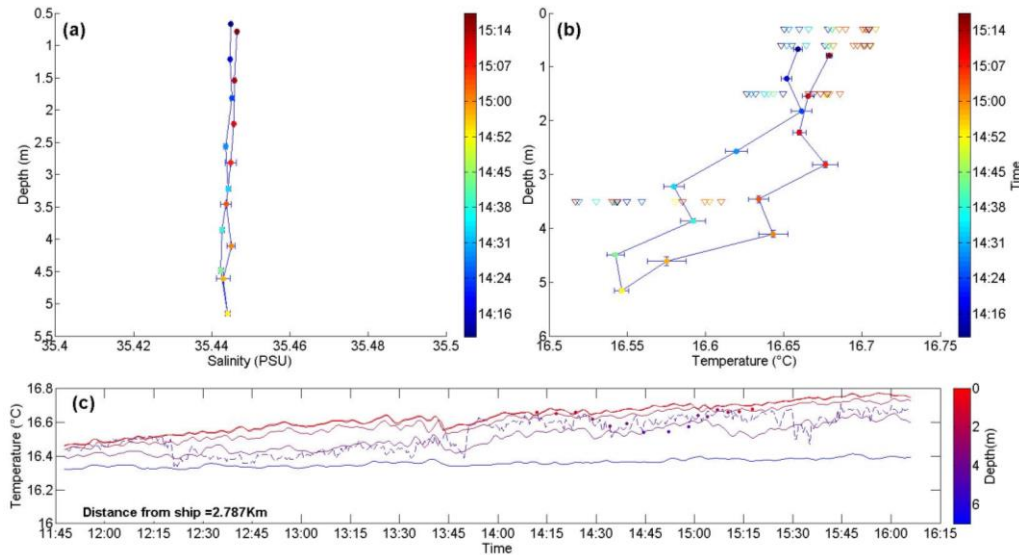


**Figure 76:** Salinity and temperature in the Central Celtic Sea on 30<sup>th</sup> July 2015. NSOP profiles of salinity (a) and temperature (b) were derived using depth bins as described in Section 2.6. Data points are coloured by sampling time. Vertical and horizontal error bars show two standard errors of the mean in each depth bin. Coloured triangles in (B) are time-



1 averaged temperature for four depths (0.3, 0.6, 1.5 and 3.5 m) at the nearby Central Celtic Sea  
2 temperature mooring (49.403°N, -8.606°E). (c) Timeseries of temperature at the mooring.  
3 Timeseries of temperature at depths (0.3, 0.6, 1.5 and 3.5 m) are solid lines whereas the  
4 dashed line is the underway temperature at 5.5 m from RRS Discovery (located 2.8 km from  
5 the mooring). The mooring and underway temperatures are coloured according to their sample  
6 depth, where red is the air/sea interface. The Coloured circles are binned temperature data  
7 from NSOP which have also been coloured to reflect the depth of collection. Sample depth is  
8 indicated by blue red colour, where red is the air/sea interface.

10 Seawater density (Fig. 8a7a) was calculated using the salinity and temperature profile data  
11 (Fig. 7a-6a & 7b6b) and the 1983 Unesco equation of state (Millero and Poisson, 1981). As  
12 expected with little variation in the salinity, changes in the density profile are dominated by  
13 temperature. The down and up casts for CO<sub>2</sub> show excellent agreement below 2.5 m. Surface  
14 water (< 2 m) CO<sub>2</sub> is 2-4 µatm higher than at 5 m (Fig. 8b7b). Elevated surface CO<sub>2</sub> could be  
15 explained by a sustained flux from the atmosphere into a near surface stratified layer with  
16 inhibited deep water exchange. Under this assumption a vertical gradient in seawater CO<sub>2</sub>  
17 would need to be established shortly after the temperature gradient. A paired t-test showed  
18 that the CO<sub>2</sub> measured in the surface bins on the downcast and upcast are were significantly  
19 different (p = <0.001). Surface CO<sub>2</sub> is significantly different between the down and up casts.  
20 The deepening of the surface stratified layer could explain the more homogeneous CO<sub>2</sub> during  
21 the upcast. It is worth noting that in addition to physical processes, plankton trapped within  
22 the surface layer could also modify the surface CO<sub>2</sub>. Trace gas concentrations may also be  
23 different in the sea surface microlayer but sampling that close to the surface is beyond the  
24 capabilities of NSOP. Complimentary measurements of the sea surface microlayer could be  
25 made using other state of the art purpose built sampling platforms such as the Sea Surface  
26 Scanner (Ribas-Ribas et al., 2017).

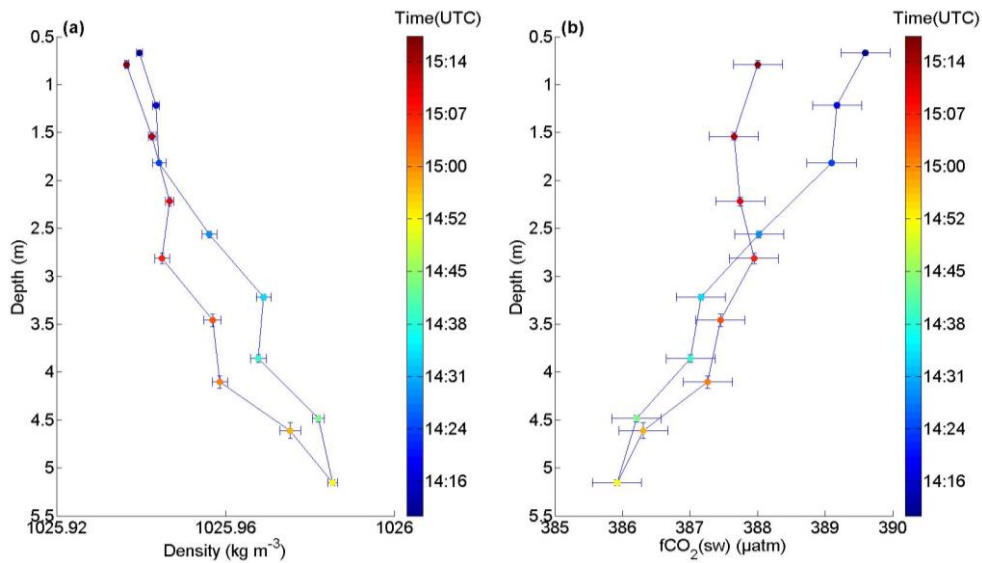


**Figure 87:** NSOP density (a) and  $\text{fCO}_2(\text{sw})$  (b) profiles from the Celtic Sea on 30<sup>th</sup> July 2015. Data points are coloured by sample time. Vertical error bars correspond to two standard errors of the mean in each depth bin. The horizontal error bars in (a) are two standard errors of the mean, whereas in (b) they are the propagated error from the the binned measurements used to calculate  $\text{fCO}_2(\text{sw})$ .

To assess measurement accuracy the NSOP Liqui-Cel  $\text{CO}_2$  system was compared against an independent  $\text{CO}_2$  system that had a showerhead equilibrator coupled to the ship's seawater supply pumped from 5.5 m below the sea surface (Hardman-Mountford et al., 2008; Kitidis et al., 2012). Technical issues meant that the underway  $\text{CO}_2$  system installed on the *RRS Discovery* was not functioning during the deployment detailed above. However during a deployment on the 19<sup>th</sup> July 2015, the  $\text{fCO}_2(\text{sw})$  measured by NSOP at 5 m agreed well with independent measurements from the underway system, difference =  $1.7 \pm 4.18 \mu\text{atm}$ . The agreement between the two systems is in line with previous intercomparisons (Royer et al., 2016; Ribas-Ribas et al., 2014) (Ribas-Ribas et al., 2014; Körtzinger et al., 2000). However during deployments on the 19<sup>th</sup> and 20<sup>th</sup> July, the  $\text{fCO}_2(\text{sw})$  measured by NSOP close to the underway intake depth agrees to within  $3 \mu\text{atm}$ .

### 3.2 Coastal deployment

DMS profiles were collected on a small research vessel on 15<sup>th</sup> April 2014. NSOP was deployed within the Plymouth Sound at 12:00 hrs UTC and recovered 95 minutes later (Fig. 10g). In the sheltered environment behind the breakwater the standard deviation in depth was  $\pm 0.10$  m, smaller than observed during open ocean profiles. Seawater temperature and salinity demonstrate clear structure, with lower temperatures and higher salinities associated with sub-surface water. Two river estuaries (Plym and Tamar) converge and flow out to the open ocean through the Plymouth Sound. We likely observed a freshwater surface lens that was protected from wave-driven mixing and had been warmed over the course of the day. We used a different miniCTD during this deployment and were thus also able to collect fluorescence data (Fig. 10d). Temperature profiles (Fig. 11a) show a sharp discontinuity in the downcast at ~5 m whereas in the upcast the thermocline had shoaled to ~3.5 m. The salinity profiles suggest similar mixing depths to the temperature profiles, with lower salinity water at the surface (Fig. 10b). ~~Fluorescence increases with depth (Fig. 10c), but this is likely due to quenching of the phytoplankton photosynthetic apparatus at the surface (Smyth et al., 2004). The increase in fluorescence with depth (Fig. 9c) is either due to reductions in chlorophyll concentration close to the sea surface or because of quenching of the phytoplankton photosynthetic apparatus, which is often observed in surface waters that experience strong irradiance (Sackmann et al., 2008).~~ DMS concentrations reduce steadily with depth (Fig. 10d), which is likely explained by changes in DMS production and consumption rates by the biological community (Galí et al., 2013). The DMS profiles from the upcast and the downcast are very similar, with the largest difference at the very surface. A large difference in the surface-most data point can also be seen in the temperature data, and may reflect mixing with sub-surface waters due to the motion of NSOP or short time-scale variations in the physical environment.

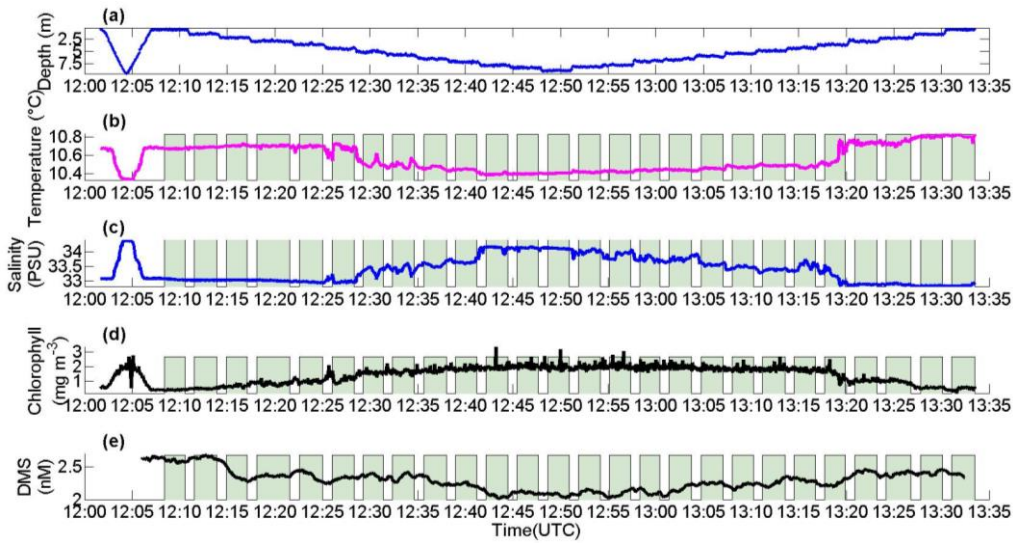


**Figure 98:** Time series measurements during an NSOP deployment in Plymouth Sound on 15<sup>th</sup> April 2014: depth (a), temperature (b), salinity (c), chlorophyll fluorescence (d) and DMS<sub>(sw)</sub> (e). Data used for depth bin analysis (Section 2.6) is identified by a shaded background. The beginning of the time series is an example off a continuous profile (see Section 2.2).

Formatted: Font: Times New Roman

Formatted: Font: Times New Roman, Not Bold

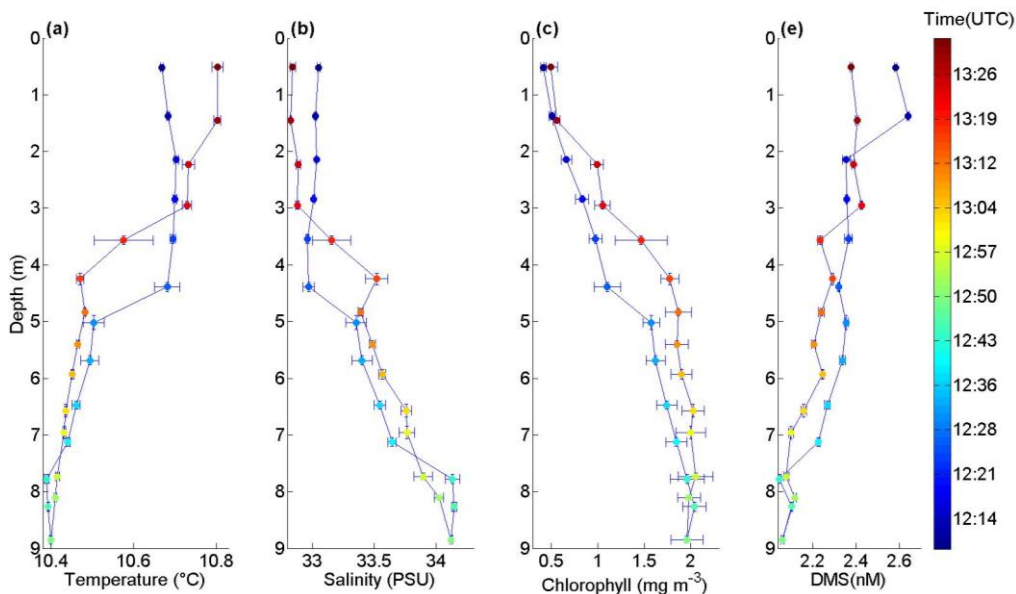


**Figure 109:** NSOP profiles collected in Plymouth Sound on 15<sup>th</sup> April 2014: temperature (a), salinity (b), chlorophyll fluorescence (c), and DMS<sub>(sw)</sub> (d). Data are coloured by sample time.

Vertical and horizontal error bars are two standard errors of the mean (SEM) in each depth bin.

#### 4 Summary

This paper describes a Near Surface Ocean Profiler (NSOP) designed to measure vertical trace gas profiles near the air-sea interface. NSOP is unique in approach as its sampling frame is lowered from a buoy that rides the ocean swell, reducing relative motion of the frame and hence fluctuations in sampling depth. The NSOP design facilitates near surface (< 0.5 m) sampling, significantly improving the capability to resolve vertical gradients. Other benefits include the ability to sample away from ship-driven turbulence and the flexibility to make a large range of near surface measurements. The NSOP sampling frame houses the miniCTD and also has the capacity to incorporate additional sensors (e.g. turbulence, dissolved oxygen and other measures of phytoplankton abundance and photosynthetic health). The ability to collect water from discrete depths facilitates the collection of near surface samples that require additional processing or take longer to analyse (e.g. TA, dissolved inorganic carbon, nutrients, the DMS-precursor DMSP, dissolved organic carbon). NSOP is highly versatile and can be used for continuous or discrete profiling. Further development could adjust winch payout speed and enable continuous, high resolution depth profiles for slower response time measurements (e.g.  $f\text{CO}_{2(\text{sw})}$ ).

Near surface stratification in the upper few metres of the ocean due to temperature and salinity gradients is a well-documented phenomenon. The presence or absence of chemical and biological gradients within near surface stratified layers has been difficult to assess. NSOP is a platform with the capability to successfully resolve gradients in these near surface layers. The data presented in this paper demonstrate that near surface gradients in trace gases can lead to substantially different fluxes depending upon the seawater depth that is used to calculate the flux. Assuming that the effect of temperature and salinity gradients on the flux can be accounted for using remote sensing methods (e.g. Shutler et al., 2016), then the change in flux is directly proportional to the change in  $\Delta C$ . In the case of the coastal DMS profile, a higher concentration (2.6 nM) was observed 0.5 m below the sea surface compared to concentrations at 5 m (2.4 nM). Assuming that the atmospheric concentration of DMS was zero (a typical approach for DMS fluxes, (see Lana et al., 2011) this will result in a corresponding flux increase of 10 %. In the case of the Celtic Sea  $\text{CO}_2$  profile, the

concentration at 0.5 m (389.6  $\mu\text{atm}$ ) was higher than at 5 m (385.9  $\mu\text{atm}$ ). The atmospheric  $\text{CO}_2$  concentration was 398.1  $\mu\text{atm}$ , which means that the surface water was less undersaturated than implied by the seawater concentration at 5 m. Thus the  $\Delta C$  and calculated air-to-sea flux are lower by 30%. The magnitude of these concentration gradients are significant, but it is unlikely that the gradients we observed will persist for all hours of the day, under different environmental conditions and in all regions of the global ocean. A subsequent publication is planned that discusses four cruises where NSOP was deployed as well as the wider prevalence and implications of near surface  $\text{CO}_2$  gradients.

~~Near surface stratification in the upper few metres of the ocean due to temperature and salinity gradients is a well documented phenomenon. The presence or absence of chemical and biological gradients within near surface stratified layers has been difficult to assess. NSOP is a platform with the capability to successfully resolve gradients in these near surface layers.~~

## Acknowledgements

We thank the captains and crews of the *RV Plymouth Quest* and *RRS Discovery* for their assistance with deploying NSOP, Christopher Balfour and Dave Sivyer for maintenance of the Central Celtic Sea mooring near surface temperature sensors, Vassilis Kitidis for supplying underway  $\text{CO}_2$  data and Burke Hales for advice concerning Liqui-Cel  $\text{CO}_2$  measurements. This research was made possible by PML internal funding, a NERC funded studentship (NE/L000075/1), temperature sensors on the Central Celtic Sea mooring (NE/K002058/1) and by the NERC Shelf Sea Biogeochemistry pelagic research programme (NE/K002007/1). The *RRS Discovery* underway data was supplied by the Natural Environment Research Council.

## References

- Bakker, D. C., Pfeil, B., Landa, C. S., Metzl, N., O'Brien, K. M., Olsen, A., Smith, K., Cosca, C., Harasawa, S., and Jones, S. D.: A multi-decade record of high-quality  $\text{fCO}_2$  data in version 3 of the Surface Ocean  $\text{CO}_2$  Atlas (SOCAT), *Earth System Science Data*, 8, 383, 2016.
- Bange, H. W., Bell, T. G., Cornejo, M., Freing, A., Uher, G., Upstill-Goddard, R. C., and Zhang, G.: MEMENTO: a proposal to develop a database of marine nitrous oxide and methane measurements, *Environmental Chemistry*, 6, 195-197, 2009.

1 Bell, T., De Bruyn, W., Miller, S., Ward, B., Christensen, K., and Saltzman, E.: Air-sea  
2 dimethylsulfide (DMS) gas transfer in the North Atlantic: evidence for limited interfacial gas  
3 exchange at high wind speed, *Atmospheric Chemistry and Physics*, 13, 11073-11087, 2013.

4 Bell, T., De Bruyn, W., Marandino, C. A., Miller, S., Law, C., Smith, M., and Saltzman, E.:  
5 Dimethylsulfide gas transfer coefficients from algal blooms in the Southern Ocean,  
6 *Atmospheric Chemistry and Physics*, 15, 1783-1794, 2015.

7 Dickson, A. G., Sabine, C. L., and Christian, J. R.: Guide to best practices for ocean CO<sub>2</sub>  
8 measurements, 2007.

9 Donlon, C., Minnett, P., Gentemann, C., Nightingale, T., Barton, I., Ward, B., and Murray,  
10 M.: Toward improved validation of satellite sea surface skin temperature measurements for  
11 climate research, *Journal of Climate*, 15, 353-369, 2002.

12 Durham, W. M., Kessler, J. O., and Stocker, R.: Disruption of vertical motility by shear  
13 triggers formation of thin phytoplankton layers, *Science*, 323, 1067-1070, 2009.

14 Fairall, C., Bradley, E. F., Godfrey, J., Wick, G., Edson, J. B., and Young, G.: Cool-skin and  
15 warm-layer effects on sea surface temperature, *Journal of Geophysical Research*, 101, 1295-  
16 1308, 1996.

17 Frankignoulle, M., and Borges, A. V.: European continental shelf as a significant sink for  
18 atmospheric carbon dioxide, *Global Biogeochemical Cycles*, 15, 569-576, 2001.

19 Galí, M., Simó, R., Vila-Costa, M., Ruiz-González, C., Gasol, J. M., and Matrai, P.: Diel  
20 patterns of oceanic dimethylsulfide (DMS) cycling: Microbial and physical drivers, *Global  
21 Biogeochemical Cycles*, 27, 620-636, 2013.

22 Hales, B., Chipman, D., and Takahashi, T.: High-frequency measurement of partial pressure  
23 and total concentration of carbon dioxide in seawater using microporous hydrophobic  
24 membrane contractors, *Limnol. Oceanogr.: Methods* 2, 356-364, 2004.

25 Hardman-Mountford, N. J., Moore, G., Bakker, D. C., Watson, A. J., Schuster, U., Barciela,  
26 R., Hines, A., Moncoiffé, G., Brown, J., and Dye, S.: An operational monitoring system to  
27 provide indicators of CO<sub>2</sub>-related variables in the ocean, *ICES Journal of Marine Science:  
28 Journal du Conseil*, 65, 1498-1503, 2008.

29 Kitidis, V., Hardman-Mountford, N. J., Litt, E., Brown, I., Cummings, D., Hartman, S.,  
30 Hydes, D., Fishwick, J. R., Harris, C., and Martinez-Vicente, V.: Seasonal dynamics of the  
31 carbonate system in the Western English Channel, *Continental Shelf Research*, 42, 30-40,  
32 2012.

33 Körtzinger, A., Mintrop, L., Wallace, D. W., Johnson, K. M., Neill, C., Tilbrook, B., Towler,  
34 P., Inoue, H. Y., Ishii, M., and Shaffer, G.: The international at-sea intercomparison of fCO<sub>2</sub>  
35 systems during the R/V Meteor Cruise 36/1 in the North Atlantic Ocean, *Marine Chemistry*,  
36 72, 171-192, 2000.

37 Lana, A., Bell, T., Simó, R., Vallina, S. M., Ballabrera-Poy, J., Kettle, A., Dachs, J., Bopp, L.,  
38 Saltzman, E., and Stefels, J.: An updated climatology of surface dimethylsulfide  
39 concentrations and emission fluxes in the global ocean, *Global Biogeochemical Cycles*, 25,  
40 2011.

41 Le Quéré, C., Andrew, R. M., Canadell, J. G., Sitch, S., Korsbakken, J. I., Peters, G. P.,  
42 Manning, A. C., Boden, T. A., Tans, P. P., and Houghton, R. A.: Global carbon budget 2016,  
43 *Earth System Science Data*, 8, 605, 2016.

1 Liss, P. S., and Slater, P. G.: Flux of Gases across the Air-Sea Interface, *Nature*, 247, 181-  
2 184, 1974.

3 Loose, B., Stute, M., Alexander, P., and Smethie, W.: Design and deployment of a portable  
4 membrane equilibrator for sampling aqueous dissolved gases, *Water Resources Research*, 45,  
5 2009.

6 Marandino, C. A., De Bruyn, W. J., Miller, S. D., and Saltzman, E. S.: Open ocean DMS  
7 air/sea fluxes over the eastern South Pacific Ocean, *Atmos. Chem. Phys.*, 9, 345-356,  
8 10.5194/acp-9-345-2009, 2009.

9 McNeil, C. L., and Merlivat, L.: The warm oceanic surface layer: Implications for CO<sub>2</sub> fluxes  
10 and surface gas measurements, *Geophysical research letters*, 23, 3575-3578, 1996.

11 Miller, S. D., Marandino, C., and Saltzman, E. S.: Ship-based measurement of air-sea CO<sub>2</sub>  
12 exchange by eddy covariance, *Journal of Geophysical Research: Atmospheres*, 115, 2010.

13 Millero, F. J., and Poisson, A.: International one-atmosphere equation of state of seawater,  
14 *Deep Sea Research Part A. Oceanographic Research Papers*, 28, 625-629, 1981.

15 Quinn, P., and Bates, T.: The case against climate regulation via oceanic phytoplankton  
16 sulphur emissions, *Nature*, 480, 51-56, 2011.

17 Ribas-Ribas, M., Rerolle, V., Bakker, D. C., Kitidis, V., Lee, G., Brown, I., Achterberg, E. P.,  
18 Hardman-Mountford, N., and Tyrrell, T.: Intercomparison of carbonate chemistry  
19 measurements on a cruise in northwestern European shelf seas, *Biogeosciences*, 11, 4339-  
20 4355, 2014.

21 Ribas-Ribas, M., Mustaffa, N. I. H., Rahlff, J., Stolle, C., and Wurl, O.: Sea Surface Scanner  
22 (S3): A Catamaran for High-resolution Measurements of Biogeochemical Properties of the  
23 Sea Surface Microlayer, *Journal of Atmospheric and Oceanic Technology*, 2017.

24 Robertson, J. E., and Watson, A. J.: Thermal skin effect of the surface ocean and its  
25 implications for CO<sub>2</sub> uptake, *Nature*, 358, 738-740, 1992.

26 Royer, S.-J., Galí, M., Saltzman, E. S., McCormick, C. A., Bell, T. G., and Simó, R.:  
27 Development and validation of a shipboard system for measuring high-resolution vertical  
28 profiles of aqueous dimethylsulfide concentrations using chemical ionisation mass  
29 spectrometry, *Environmental Chemistry*, 11, 309-317, 2014.

30 Royer, S. J., Galí, M., Mahajan, A. S., Ross, O. N., Pérez, G. L., Saltzman, E. S., and Simó,  
31 R.: A high-resolution time-depth view of dimethylsulphide cycling in the surface sea,  
32 *Scientific Reports*, 6, 32325, 2016.

33 Saltzman, E. S., De Bruyn, W. J., Lawler, M., Marandino, C., and McCormick, C.: A  
34 chemical ionization mass spectrometer for continuous underway shipboard analysis of  
35 dimethylsulfide in near-surface seawater, *Ocean Science*, 5, 537-546, 2009.

36 Shutler, J. D., Land, P. E., Piolle, J.-F., Woolf, D. K., Goddijn-Murphy, L., Paul, F., Girard-  
37 Ardhuin, F., Chapron, B., and Donlon, C. J.: FluxEngine: A Flexible Processing System for  
38 Calculating Atmosphere–Ocean Carbon Dioxide Gas Fluxes and Climatologies, *Journal of*  
39 *Atmospheric and Oceanic Technology*, 33, 741-756, 2016.

40 Smyth, T. J., Fishwick, J. R., Lisa, A.-M., Cummings, D. G., Harris, C., Kitidis, V., Rees, A.,  
41 Martinez-Vicente, V., and Woodward, E. M.: A broad spatio-temporal view of the Western  
42 English Channel observatory, *Journal of Plankton Research*, 32, 585-601, 2010.



1 Takahashi, T., Olafsson, J., Goddard, J. G., Chipman, D. W., and Sutherland, S.: Seasonal  
2 variation of CO<sub>2</sub> and nutrients in the high-latitude surface oceans: A comparative study,  
3 *Global Biogeochemical Cycles*, 7, 843-878, 1993.

4 Turk, D., Zappa, C. J., Meinen, C. S., Christian, J. R., Ho, D. T., Dickson, A. G., and  
5 McGillis, W. R.: Rain impacts on CO<sub>2</sub> exchange in the western equatorial Pacific Ocean,  
6 *Geophysical Research Letters*, 37, 2010.

7 Walker, C. F., Harvey, M. J., Smith, M. J., Bell, T. G., Saltzman, E. S., Marriner, A. S.,  
8 McGregor, J. A., and Law, C. S.: Assessing the potential for dimethylsulfide enrichment at  
9 the sea surface and its influence on air-sea flux, *Ocean Science*, 12, 1033, 2016.

10 Wanninkhof, R.: Relationship between wind speed and gas exchange over the ocean revisited,  
11 *Limnol. Oceanogr. Methods*, 12, 351-362, 2014.

12 Ward, B., Wanninkhof, R., McGillis, W. R., Jessup, A. T., DeGrandpre, M. D., Hare, J. E.,  
13 and Edson, J. B.: Biases in the air-sea flux of CO<sub>2</sub> resulting from ocean surface temperature  
14 gradients, *Journal of Geophysical Research: Oceans* (1978–2012), 109, 2004.

15 Webb, J. R., Maher, D. T., and Santos, I. R.: Automated, in situ measurements of dissolved  
16 CO<sub>2</sub>, CH<sub>4</sub>, and δ<sup>13</sup>C values using cavity enhanced laser absorption spectrometry: Comparing  
17 response times of air-water equilibrators, *Limnology and Oceanography: Methods*, 14, 323-  
18 337, 2016.

19 Woolf, D., Land, P. E., Shutler, J. D., Goddijn-Murphy, L., and Donlon, C. J.: On the  
20 calculation of air-sea fluxes of CO<sub>2</sub> in the presence of temperature and salinity gradients,  
21 *Journal of Geophysical Research: Oceans*, 2016.

22 Yang, M., Beale, R., Smyth, T., and Blomquist, B.: Measurements of OVOC fluxes by eddy  
23 covariance using a proton-transfer-reaction mass spectrometer—method development at a  
24 coastal site, *Atmospheric Chemistry and Physics*, 13, 6165-6184, 2013.

25 Ziska, F., Quack, B., Abrahamsson, K., Archer, S., Atlas, E., Bell, T., Butler, J., Carpenter,  
26 L., Jones, C., and Harris, N.: Global sea-to-air flux climatology for bromoform,  
27 dibromomethane and methyl iodide, *Atmospheric Chemistry and Physics*, 13, 8915-8934,  
28 2013.

29

30